Sensitivity to two photon exchange in time-like form factor measurements at PANDA

Malgorzata Sudol, Thierry Hennino, Egle Tomasi-Gustafsson

Sensitivity to two photon exchange in time-like form factor measurements at PANDA

M. Sudoł, T. Hennino, and E. Tomasi-Gustafsson*

Institut de Physique Nucléaire d'Orsay, CNRS/IN2P3,

and Université Paris Sud, 91406 Orsay, France

Abstract

At $\overline{\mathrm{P}}$ANDA(FAIR) proton time-like form factors measurements are foreseen. In this work, following detailed simulations, we study the sensitivity to possible two photon exchange contributions in the annihilation process $\bar{p} + p \rightarrow e^+ + e^-$, through the induced asymmetry in the angular distribution. Asymmetries related to systematic errors are also investigated.

PACS numbers:

*IRFU/SPhN, CEA Saclay, 91191 Gif-sur-Yvette Cedex, France

Let us consider the reaction

$$\bar{p} + p \to e^+ + e^- \tag{1}$$

The expression of the hadron electromagnetic current is usually derived assuming one photon exchange (OPE). The internal structure of the hadrons is parametrized in terms of two form factors (FFs), which are complex functions of q^2, the four momentum squared of the virtual photon. Two photon exchange (TPE) is suppressed by a factor of α, the electromagnetic fine structure constant, $\alpha = 1/137$. At large q^2, however, two photon exchange could play a role, due, in particular, to a possible enhancement from a mechanism where the momentum is equally shared between the two photons. In this case, the simple formalism which allows the extraction of the electromagnetic form factors, would not hold anymore. The general analysis of experimental observables in the reaction $\bar{p}+p \to e^+ + e^-$ and in the time reversal channel, taking into account the TPE contribution, was done in Ref. [1], according to a model independent formalism developed for elastic electron proton scattering [2].

In particular, it has been shown that instead of two amplitudes, functions of q^2, the general structure of the hadronic tensor contains five amplitudes, when one considers the TPE contribution.

The differential cross section of the reaction (1) for the case of unpolarized particles has the form:

$$\frac{d\sigma}{d\Omega} = \frac{\alpha^2}{4q^2}\sqrt{\frac{\tau}{\tau-1}}D,\ \tau = \frac{q^2}{4m^2}, \tag{2}$$

$$\begin{aligned} D \ = \ & (1+\cos^2\theta)[|G_M|^2 + 2(ReG_M\Delta G_M^*)] + \frac{1}{\tau}\sin^2\theta[|G_E|^2 + 2Re(G_E\Delta G_E^*)] + \\ & 2\sqrt{\tau(\tau-1)}\cos\theta\sin^2\theta Re(\frac{1}{\tau}G_E - G_M)F_3^*. \end{aligned} \tag{3}$$

where we have defined the following decomposition of the amplitudes:

$$\tilde{G}_M(q^2,t) = G_M(q^2) + \Delta G_M(q^2,t),\ \tilde{G}_E(q^2,t) = G_E(q^2) + \Delta G_E(q^2,t). \tag{4}$$

where $\Delta G_{E,M}$ corresponds to the TPE contribution to $G_{E,M}$ and F_3 is entirely due to TPE. We neglect below the bilinear combinations of the terms ΔG_M, ΔG_E and F_3 since they are smaller (at least of the order of α), in comparison with the dominant ones.

Symmetry properties of the amplitudes with respect to the $\cos\theta \to -\cos\theta$ transformation can be derived from the C invariance of the considered $1\gamma \otimes 2\gamma$ mechanism:

$$\Delta G_{M,E}(\cos\theta) = -\Delta G_{M,E}(-\cos\theta),\ F_3(\cos\theta) = F_3(-\cos\theta). \tag{5}$$

One can see that in the Born approximation the expression (3) reduces to the result firstly obtained in Ref. [3]:

$$D = (1 + \cos^2\theta)|G_M|^2 + \frac{1}{\tau}\sin^2\theta|G_E|^2. \quad (6)$$

The contribution of the OPE diagram leads to an even function of $\cos\theta$, whereas the TPE contribution leads to four new terms of the order of α compared to the dominant contribution. Different properties of the observables are described in detail in Ref. [1]. Here let us recall that, at the reaction threshold $q^2 = 4m^2$, from which one gets $G_M = G_E$ and the differential cross section becomes $\theta-$independent in the Born approximation. This is not anymore true in presence of TPE terms. Note also that the contribution to the cross section due to TPE, being an odd function of the variable $\cos\theta$, does not contribute to the differential cross section for $\theta = 90^0$.

I. ANALYSIS OF THE DATA

Angular distributions are simulated according to Eqs. (2) and (6), assuming $|G_E| = |G_M|$ for three values of q^2=5.4, 8.2 and 13.6 GeV^2, and a luminosity of $\mathcal{L} = 2 \cdot 10^{32}$ cm^{-2}s^{-1}, including the detector efficiency. Histograms are built as functions of $\cos\theta$, in 0.2 wide bins. The experimental conditions are shown in Table I. The total number of counts is calculated assuming 120 days of measurement. In case of two photon exchange, the amplitudes (ΔG_E, ΔG_M, F_3), are not known. Therefore we will use the presence of odd terms in $\cos\theta$ as a (model independent) signature of TPE and approximate Eq. (3) by

$$D \simeq (1 + \cos^2\theta)|G_M|^2 + \frac{1}{\tau}\sin^2\theta|G_E|^2 + 2\sqrt{\tau(\tau-1)}\cos\theta\sin^2\theta(\frac{1}{\tau}G_E - G_M)F_3. \quad (7)$$

Eq. (7) contains drastic approximations: we neglect the contributions $\Delta G_{E,M}$ which, in any case, can not be inferred from unpolarized measurements. Then, in the last term, we consider only the real part of F_3, G_E, and G_M, as their relative phases are not known. The purpose is to see up to which limit an odd $\cos\theta$ contribution can be extracted from the data. Eq. (7) contains odd $\cos\theta$ terms of first and third order. To start with, we neglect the $\cos^3\theta$ term. In a second step, we give the results including the linear and the cubic terms.

For the three values of q^2 given above, we have simulated distributions according to Eq. (7), with $|G_E| = |G_M|$ and F_3/G_M=0.02, 0.05 and 0.2. The asymmetry induced by these

components can be seen in Fig. 1, where the angular distributions are shown as a function of $\cos\theta$. One can see that as one moves from no contribution (black circles), to 2% contribution (red squares), 5% contribution (green triangles) 20% contribution (blue triangle down), the vertex moves on the left side (it depends on the sign of the coefficient of the $\cos\theta$ term) and the distribution becomes more and more asymmetric, with respect to $\cos\theta = 0$, being still a parabola. Including a $\cos^3\theta$ term makes a different distorsion of the distribution. As we keep the same coefficients for the linear and cubic terms, such distorsion cancels at $\cos\theta$=0 and $\pm$ 1, see Fig. 2.

In order to analyze the distributions, and extract the values of the two photon amplitude, we rewrite the angular distribution as a polynomial in $\cos\theta$. One can see that in case of OPE, Eqs. (2) and (6), can be rewritten as

$$\frac{d\sigma}{d(\cos\theta)} = \sigma_0 \left[1 + \mathcal{A}\cos^2\theta\right], \tag{8}$$

where

$$\sigma_0 = \frac{\alpha^2}{4q^2}\sqrt{\frac{\tau}{\tau-1}}\left(|G_M|^2 + \frac{1}{\tau}|G_E|^2\right) \tag{9}$$

is the value of the differential cross section at $\theta = \pi/2$ and $\mathcal{A}$ can be written as a function of the FFs:

$$\mathcal{A} = \frac{\tau|G_M|^2 - |G_E|^2}{\tau|G_M|^2 + |G_E|^2} = \frac{\tau - \mathcal{R}^2}{\tau + \mathcal{R}^2}. \tag{10}$$

where $\mathcal{R} = |G_E|/|G_M|$.

Therefore, at each value of q^2, we can fit the angular distributions with a straight line in $\cos^2\theta$,

$$y = a_0 + a_1 x \text{ with } x = \cos^2\theta,\ a_0 \equiv \sigma_0,\ a_1 \equiv \sigma_0\mathcal{A} \tag{11}$$

a_0 and a_1 are related to the physical FFs, through Eqs. (9) and (10).

Deviations from a straight line will be evidence of the presence of higher order terms, beyond Born approximation. Such C-odd terms appear as functions of $\cos\theta$. We can fit the distributions by a quadratic function (neglecting, as a first step, $\cos^3\theta$):

$$y = a_0 + a_2 x' + a_1 x'^2,\ x' = \cos\theta, \tag{12}$$

or including $\cos^3\theta$, with the same three parameters:

$$y = a_0 + a_2(x' - x'^3) + a_1 x'^2,\ x' = \cos\theta, \tag{13}$$

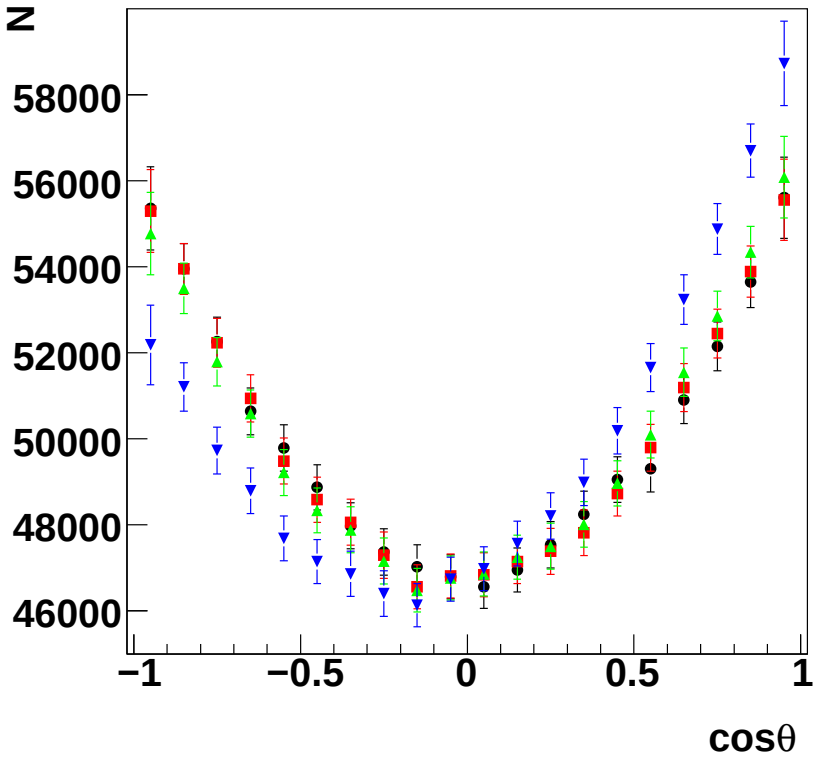

FIG. 1: Angular distributions for different contribution of TPE (including only the $\cos\theta$ term at $q^2 = 5.4$ GeV^2: no contribution (black circles), 2% contribution (red squares), 5% contribution (green triangles) 20% contribution (blue triangledown).

with

$$a_2 \equiv \frac{2\sqrt{\tau(\tau-1)}(G_E - \tau G_M)F_3}{\tau|G_M|^2 + |G_E|^2}. \tag{14}$$

These last fits are performed with MINUIT.

s [GeV ^{2}]	E [GeV]	p	σ [pb]	Events
5.4	1.	1.7	538	1.1 10^6
8.2	2.5	3.3	32	6.4 10^4
13.8	5.47	5.86	1	2 10^3

TABLE I: Expected counting rates, for $\overline{p} + p \to e^+ + e^-$.

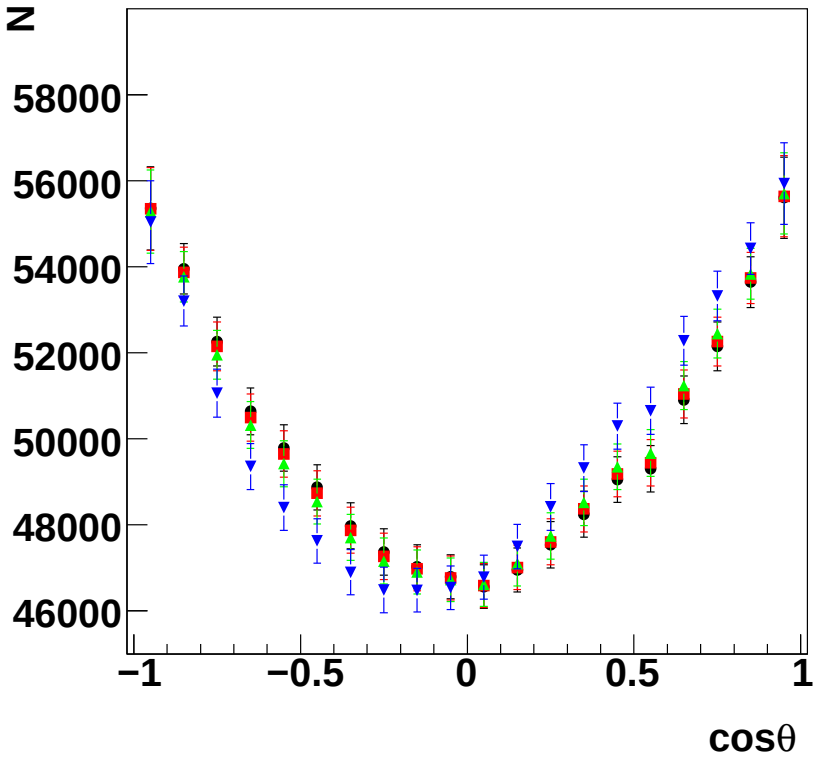

FIG. 2: Same as Fig. 1, including the cubic term.

II. RESULTS

The results of the fit are reported in Table II, in the case where we neglect the cubic term. We can see that, for the 1γ spectra, as expected, the coefficient a_2 is compatible with zero, for all q^2 values, its value being inferior to the other parameters. The odd $\cos\theta$ contribution starts to be visible for $F_3/G_M \geq 5\%$. Note however that the extraction of $\mathcal{R}$ and $\mathcal{A}$ is not affected, in the limit of the error bars, by the presence of the C-odd term. The differential cross section is a quadratic function (parabola) in $\cos\theta$. The linear $\cos\theta$ term is related to the position of the vertex of the parabola, a TPE contribution corresponds to a shift of this vertex. Therefore, the quadratic and constant coefficient are very stable. Only for the largest 2γ contribution, a systematic deviation of the reconstructed values of $\mathcal{R}$ and $\mathcal{A}$ from the input ones is observed. If one uses a two parameter fit, in presence of TPE, (Table III) the χ^2 becomes worse. Fig. 3 shows the angular distribution as a function of $\cos^2\theta$. The lower (upper) branches correspond to backward (forward) emission for a negative lepton.

The solid (black) line is the result of the quadratic fit, the dashed (blue line) is the result of the linear fit.

Including the $\cos^3\theta$ term changes indeed the angular distributions, in particular canceling the distortion for collinear kinematics (where it is maximum in the previous case). However the previous conclusions do not change, as it is shown in Fig. 4 for the lowest q^2 value, in Fig. 5 for all considered cases, and in table IV, for the lowest value of q^2: the parameter a_2 shows a sensitivity to TPE starting from F_3/G_M=0.05. The linear fit shows less deviation and a better χ^2 than in the case where only the linear $\cos\theta$ term is kept: the distortion from a parabola cancels for collinear kinematics, and for $\cos\theta = 0$, see Table V.

III. EXPERIMENTAL ASYMMETRIES

Experimental bias, as possible misalignments of the detectors, approximations in the algorithms for reconstruction..., can appear as a distortion of the angular distribution, which translates into systematic errors. The experimental angular distribution can always be fitted by a function decomposed in a Fourier series of sines and cosines. In this section we look to the sensitivity to a sine term. Histograms are built according to a distribution obtained by adding a term $C\sin\theta$ to Eq. (6), the expression which corresponds to one photon approximation. Numerical estimations have been done for different values of $C\sin\theta$ (C=0,0.002,0.004,0.02) and the corresponding angular distributions are reported in Fig. 6. The values of the coefficient C have been chosen in order to have a reasonable size of this term as compared to the two photon case. Similarly to the TPE case, the distributions have been fitted by the function:

$$y = a_0 + a_1\cos^2\theta + C\sin\theta. \tag{15}$$

The values of the parameters, as well as the extracted $\mathcal{R}$ and $\mathcal{A}$ are reported in table VI. The quality of the fit can be seen in Fig. 6.

The results look very different from the previous cases, although the values of C are such to induce a quantitative comparable perturbation to the OPE distribution as in the previous section. Evidently the effect of the sine term is to induce a modulation in the distribution according to the angles: minimal for θ=0 and 180 degrees, maximal for θ=90 degrees. However, this distortion has the same sign for forward and backward angles as the

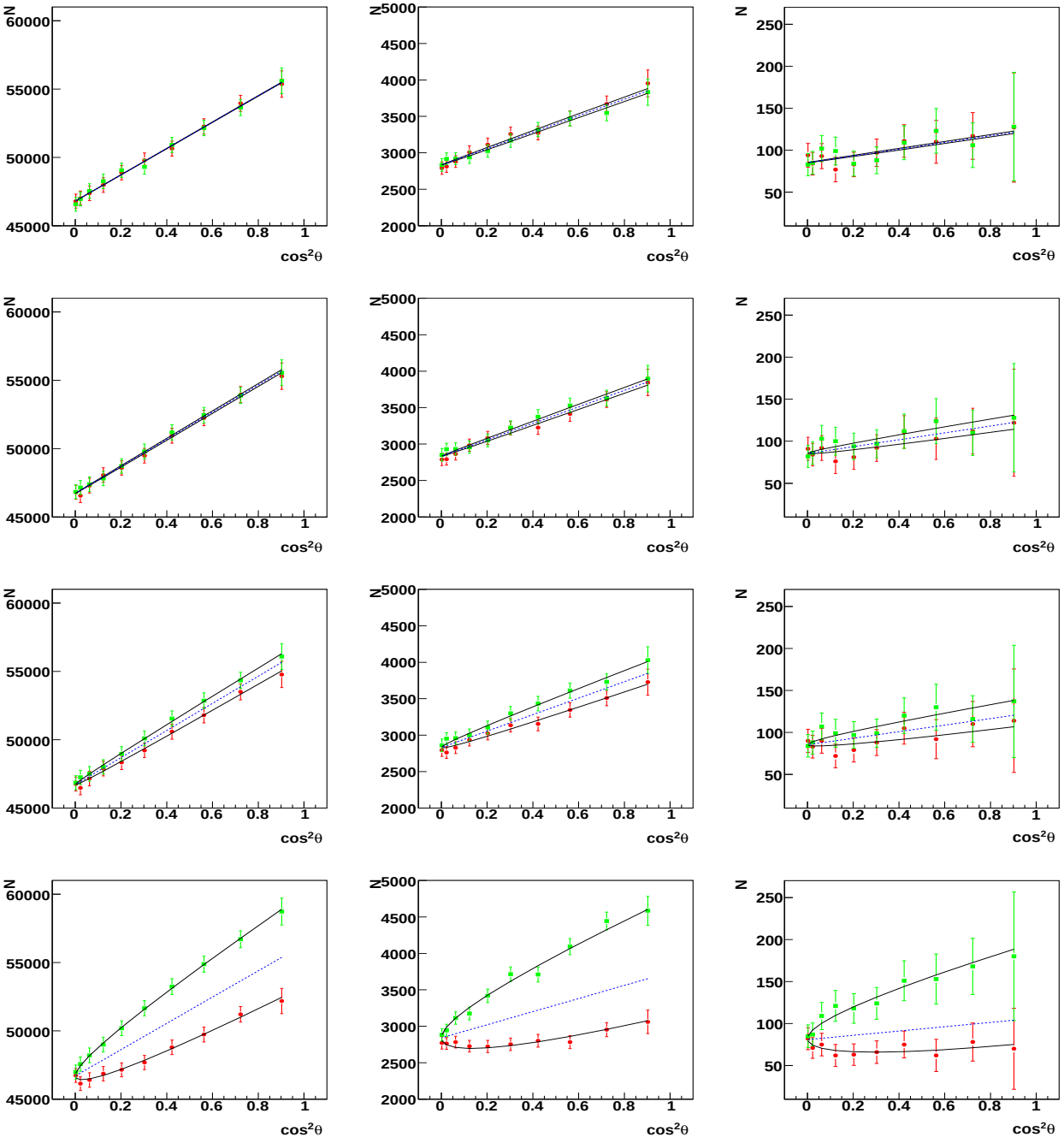

FIG. 3: Angular distributions as a function of $\cos^2\theta$, built according to 7, but including only the linear $\cos\theta$ term, for different contribution of TPE: from top to bottom: no contribution, 2% contribution , 5% contribution, 20% contribution and for different q^2 values : from left to right q^2=5.4, 8.2 and 13.6 GeV^2. Backward scattering (green points), forward scattering (red points). The solid (black) line correspond to the quadratic fit (12), the dashed (blue line) to the linear fit (11).

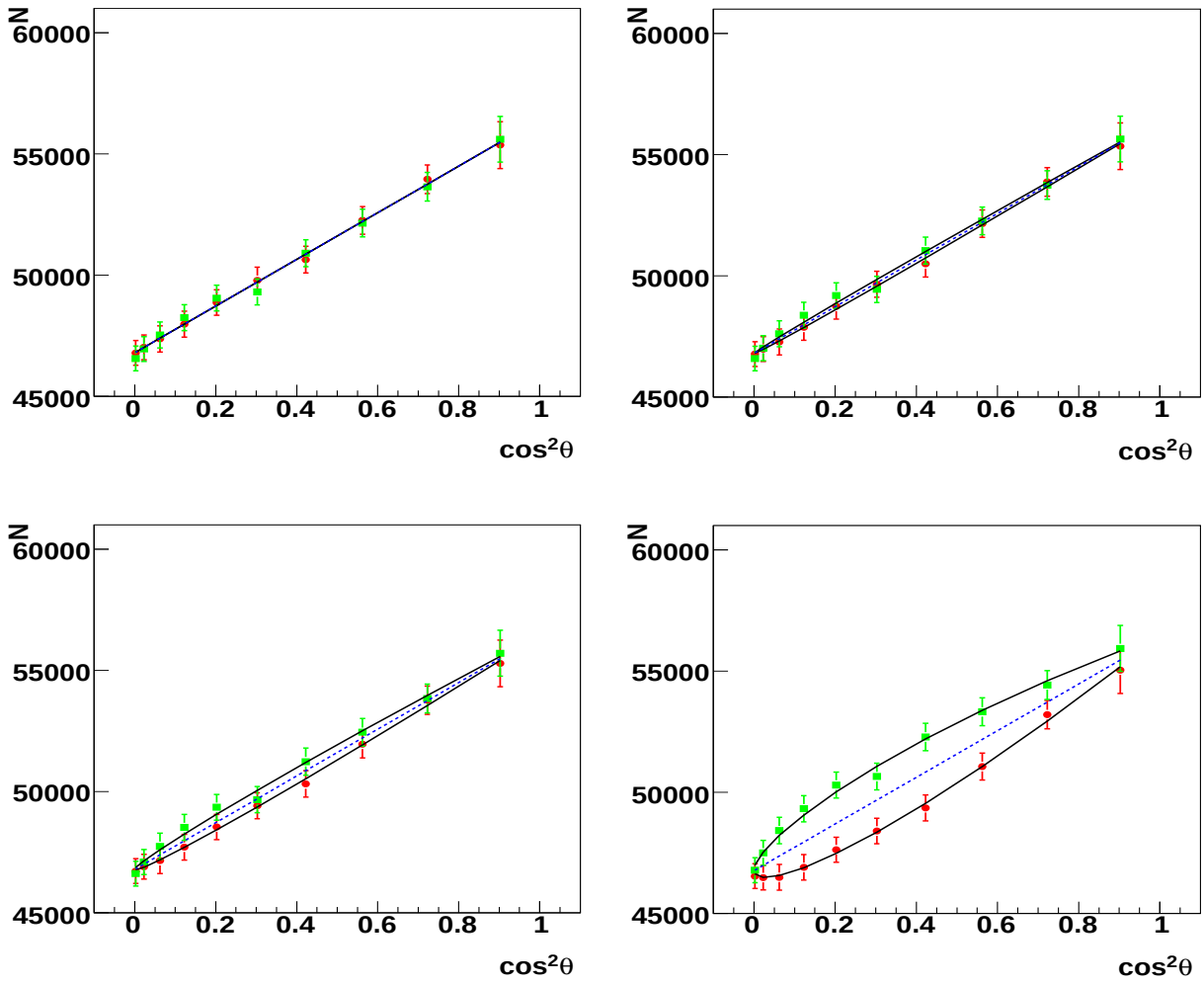

FIG. 4: Angular distributions as functions of $\cos^2\theta$, according to Eq. (7), for q^2 =5.4 GeV^2 and for different contribution of TPE : no contribution (top left), 2% contribution (top right), 5% contribution (bottom left), and 20% contribution (bottom right). Notations as in Fig. 3.The solid (black) line correspond to the cubic fit (13), the dashed (blue line) to the linear fit (11).

main amplitudes (square of cosine and sine), therefore it is much more difficult to identify and extract it with a fitting procedure. One can see that the adding a sine term in the function, the error on the parameters becomes very large, even when the coefficient is zero. Perturbations on the the values obtained in the linear fit (taking into account the error of the linear fit) can be seen even for no sine contribution.

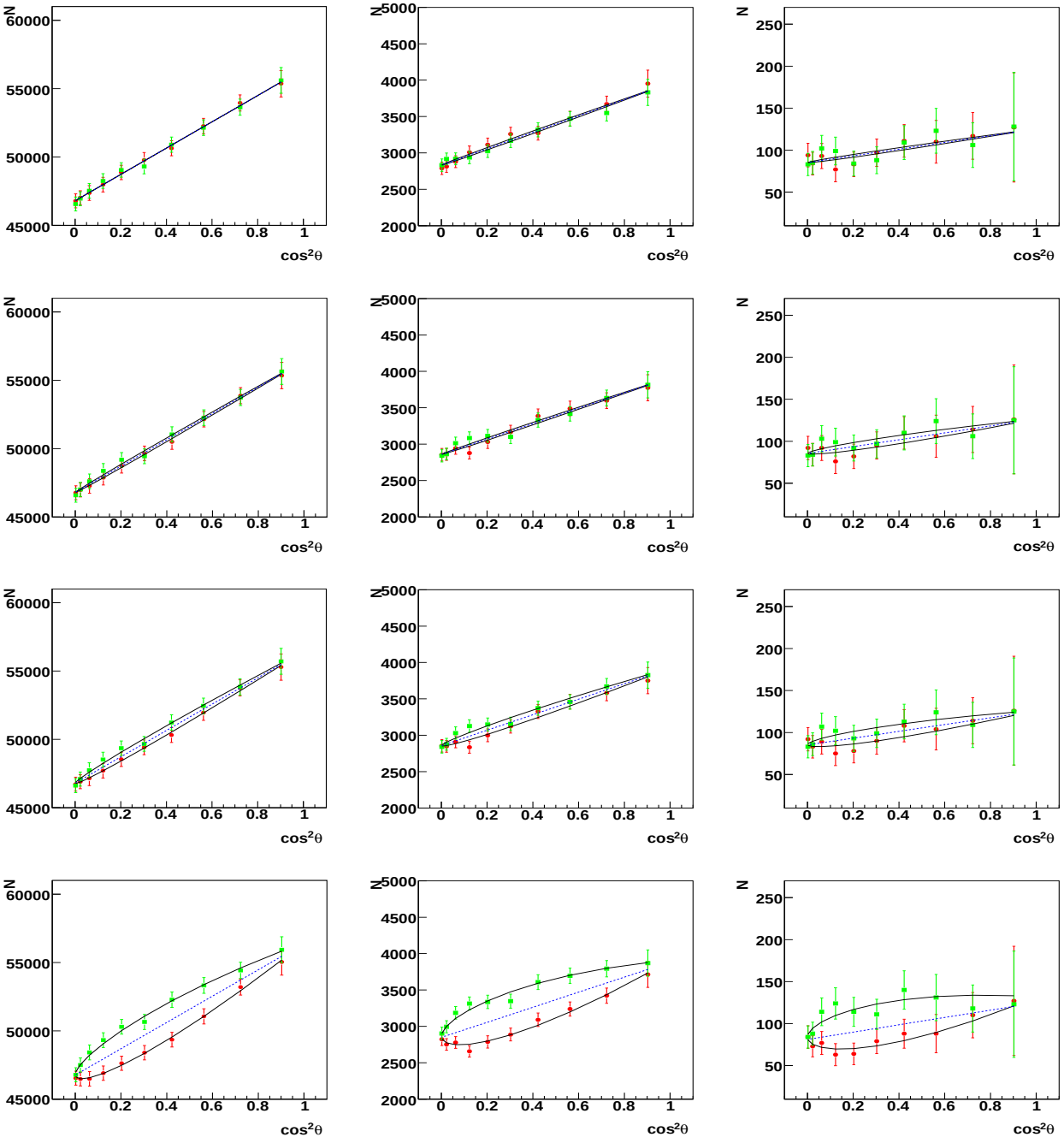

FIG. 5: Angular distributions as functions of $\cos^2\theta$, according to Eq. 7 for different contribution of TPE: from top to bottom : no contribution, 2% contribution , 5% contribution, 20% contribution and for different q^2 values : from left to right q^2=5.4, 8.2 and 13.6 GeV^2.Notations as in Fig. 3. The solid (black) line corresponds to the cubic fit (13), the dashed (blue line) to the linear fit (11).

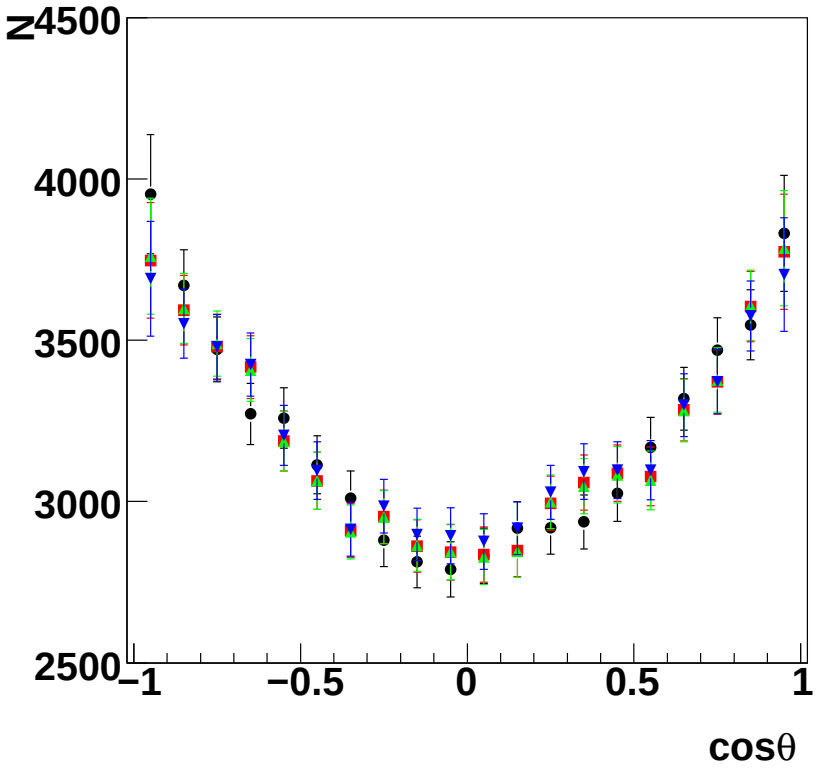

FIG. 6: Angular distributions for different additional $C \sin\theta$ contributions at $q^2 = 8.4$ GeV^2: no contribution (black circles), $C = 0.2\%$ contribution (red squares), $C = 0.4\%$ contribution (green triangles), and $C = 2\%$ contribution (blue triangle down). Notations as in Fig. 3.

IV. CONCLUSIONS

We have shown that the PANDA experiment will be sensitive to a contribution of TPE of 5% or more. TPE contribution is expected to increase at large q^2, where the statistical error is also expected to be larger, making more difficult its extraction. Due to crossing symmetry properties, the reaction mechanism should be the same in SL and TL regions. If TPE is the reason of the discrepancy between the polarized and unpolarized FFs measurements in SL region, a contribution of 5% is necessary to bring the data in agreement, in the $|q^2|$ range between 1 and 6 GeV^2 [4]. The PANDA simulations show that such level of contribution will be detectable in the annihilation data. We have shown and discussed the stability of the extraction of $\mathcal{R}$ and $\mathcal{A}$, from the data, even in presence of a relatively large contribution of TPE.

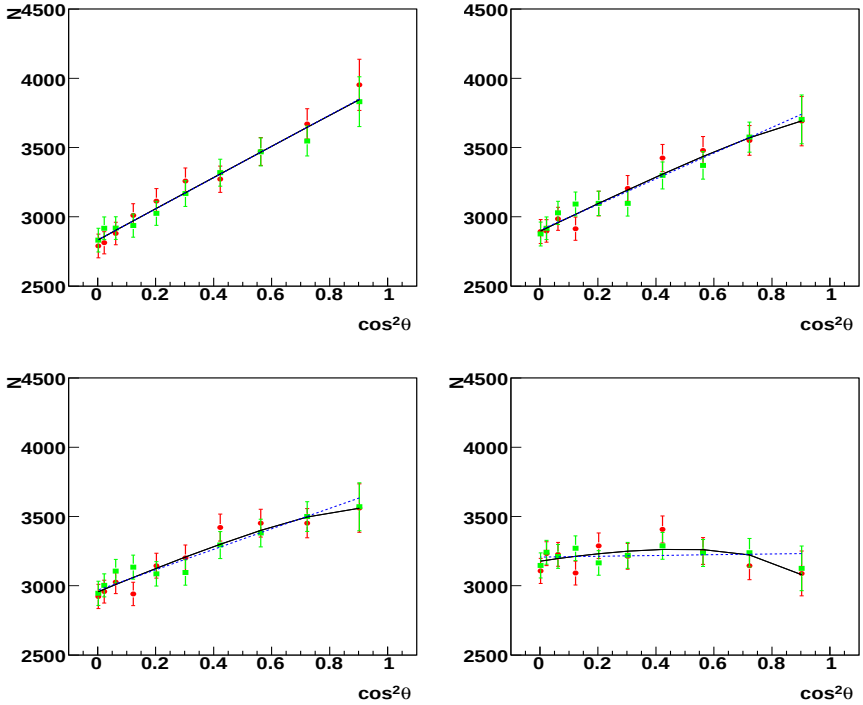

FIG. 7: $\cos^2\theta$ dependence for different contribution in $\sin\theta$ term at $q^2 = 8.4$ GeV^2: no contribution (top right),0.2% contribution (top left), 0.4% contribution (bottom right), and 2% contribution (bottom left). The solid (black) line correspond to the fit as in Eq. (15), the dashed (blue line) to the linear fit.

This has to be taken with caution, as the relation of $\mathcal{A}$ with FFs, Eq. (10), holds only in frame of OPE. The signification of the extracted $\mathcal{R}$ as the ratio of moduli of the two electromagnetic form factors is not valid anymore. $\mathcal{R}$ has to be considered, in this case, as a kind of effective parameter.

However, one should note that if one does not detect the charge of the outgoing lepton, TPE contribution cancels in the angular distributions, and that the cross section at 90° does not contain any odd contribution, by definition. TPE will cancel in the sum of the forward-backward cross section, and will appear in the forward backward asymmetry. The moduli of the FFs ratio can be extracted knowing the cross section at at least two angles, even in presence of two photon exchange. This is the main advantage of such study in the time-like region: even in presence of TPE, the angular distribution of the scattered electron pair, for one setting of the antiproton beam, contains all the useful information. In space-like region, the extraction of FFs through the Rosenbluth fit requires measurements at different angles

for the same Q^2 (i.e. it is necessary to change beam energy and detection angle at each point). In case of TPE, it is necessary to measure electron and positron scattering, in the same kinematical conditions.

One should note, however, that experimentally, no evidence of TPE (more exactly, of the real part of the interference between OPE and TPE) has been found in the experimental data on elastic scattering for spin zero [5], one half [6], and one [8]. An analysis of the BABAR data [7] does not show evidence of two photon contribution, in the limit of the uncertainty of the data [9].

We studied also the distortion induced by a sine term. In this case the results of the fit are very different, for the main parameters, even for small extra contributions.

Therefore we can conclude that a contribution of the order of 5% of two photon exchange, driven by odd terms in $\cos\theta$, will be visible. Care will have to be taken with the real data, in order to identify extra contributions which may induce distorsion in the angular distribution and make it different from the expectations given by the one photon exchange mechanism.

---

[1] G. I. Gakh and E. Tomasi-Gustafsson, Nucl. Phys. A **761**, 120 (2005);

[2] M. P. Rekalo and E. Tomasi-Gustafsson, Eur. Phys. J. A **22**, 331 (2004); Nucl. Phys. A **740**, 271 (2004); Nucl. Phys. A **742**, 322 (2004).

[3] A. Zichichi, S.M. Berman, N. Cabibbo and R. Gatto, Nuovo Cimento **XXIV**, 170 (1962).

[4] C. F. Perdrisat, V. Punjabi and M. Vanderhaeghen, Prog. Part. Nucl. Phys. **5**9, (2007) 694.

[5] G. I. Gakh and E. Tomasi–Gustafsson, arXiv:0801.4646 [nucl-th].

[6] E. Tomasi-Gustafsson and G. I. Gakh, Phys. Rev. C **72**, 015209 (2005).

[7] B. Aubert *et al.* [BABAR Collaboration], Phys. Rev. D **73**, 012005 (2006).

[8] M. P. Rekalo, E. Tomasi-Gustafsson and D. Prout, Phys. Rev. C **60**, 042202(R) (1999).

[9] E. Tomasi-Gustafsson, E. A. Kuraev, S. Bakmaev and S. Pacetti, Phys. Lett. B **659** (2008) 197.

q^2 (GeV^2)	case	a_0	a_2	a_1	χ^2	χ^2/N_f	$\mathcal{R}$	$\mathcal{A}$
5.4	1γ	46798 ± 182	-23 ± 239	9927 ± 485	1.94	0.11	1.004 ± 0.017	0.21 ± 0.01
	$2\gamma \cdot 0.02$	46713 ± 182	119 ± 240	9926 ± 485	1.45	0.09	0.997 ± 0.017	0.21 ± 0.01
	$2\gamma \cdot 0.05$	46714 ± 182	662 ± 240	9924 ± 485	1.47	0.09	0.998 ± 0.017	0.21 ± 0.01
	$2\gamma \cdot 0.20$	46710 ± 182	3398 ± 240	9933 ± 485	1.13	0.07	0.997 ± 0.017	0.21 ± 0.01
8.2	1γ	2832 ± 30	-35 ± 42	1128 ± 85	3.66	0.22	1.001 ± 0.095	0.398 ± 0.030
	$2\gamma \cdot 0.02$	2833 ± 29	45 ± 42	1130 ± 85	3.78	0.22	1.000 ± 0.095	0.399 ± 0.030
	$2\gamma \cdot 0.05$	2830 ± 30	163 ± 42	1136 ± 85	3.49	0.21	0.998 ± 0.096	0.401 ± 0.030
	$2\gamma \cdot 0.20$	2842 ± 30	805 ± 42	1106 ± 84	6.54	0.38	1.012 ± 0.092	0.389 ± 0.030
13.84	1γ	85 ± 5	2 ± 9	39 ± 19	4.49	0.26	1.149 ± 1.09	0.469 ± 0.230
	$2\gamma \cdot 0.02$	86 ± 5	9 ± 9	41 ± 19	3.36	0.19	1.133 ± 1.116	0.481 ± 0.228
	$2\gamma \cdot 0.05$	86 ± 5	16 ± 9	41 ± 19	3.67	0.22	1.137 ± 1.107	0.478 ± 0.228
	$2\gamma \cdot 0.20$	82 ± 5	59 ± 9	55 ± 18	2.12	0.12	0.848 ± 2.121	0.672 ± 0.233

TABLE II: Results from the quadratic fit, for different values of q^2 and different TPE contributions, including only the $\cos\theta$ term.

q^2 (GeV^2)	case	a_0	a_1	χ^2/N_f
5.4	1γ	46702 ± 182	9954 ± 485	0.10
	$2\gamma \cdot 0.02$	46713 ± 182	9926 ± 485	0.09
	$2\gamma \cdot 0.05$	46713 ± 182	9913 ± 485	0.5
	$2\gamma \cdot 0.20$	46700 ± 182	9611 ± 484	11.2
8.2	1γ	2832 ± 30	1127 ± 85	0.22
	$2\gamma \cdot 0.02$	2833 ± 29	1130 ± 85	0.27
	$2\gamma \cdot 0.05$	2830 ± 30	1128 ± 85	1.03
	$2\gamma \cdot 0.20$	2841 ± 30	899 ± 84	20.4
13.84	1γ	85 ± 5	40 ± 19	0.25
	$2\gamma \cdot 0.02$	85 ± 5	41 ± 19	0.19
	$2\gamma \cdot 0.05$	85 ± 5	39 ± 19	0.39
	$2\gamma \cdot 0.20$	81 ± 5	26 ± 18	2.5

TABLE III: Results from the linear fit, according to Eq. 11, on the histograms built for different values of q^2 and different TPE contributions, according to Eq. 7, but including only the $\cos\theta$ term.

q^2 (GeV^2)	case	a_0	a_2	a_1	χ^2	χ^2/N_f	$\mathcal{R}$	$\mathcal{A}$
5.4	1γ	46798 ± 182	-4 ± 442	9927 ± 485	1.94	0.11	1.004 ± 0.017	0.21 ± 0.01
	$2\gamma \cdot 0.02$	46795 ± 182	361 ± 442	9638 ± 485	1.96	0.11	1.004 ± 0.017	0.21 ± 0.01
	$2\gamma \cdot 0.05$	46795 ± 182	891 ± 442	9636 ± 485	1.82	0.11	1.004 ± 0.017	0.21 ± 0.01
	$2\gamma \cdot 0.20$	46789 ± 182	3537 ± 442	9657 ± 485	2.01	0.12	1.003 ± 0.017	0.21 ± 0.01
8.2	1γ	2832 ± 30	-45 ± 74	1127 ± 85	3.96	0.23	1.001 ± 0.095	0.398 ± 0.030
	$2\gamma \cdot 0.02$	2859 ± 30	45 ± 75	1057 ± 85	6.29	0.37	1.036 ± 0.087	0.369 ± 0.030
	$2\gamma \cdot 0.05$	2830 ± 30	163 ± 42	1136 ± 85	5.92	0.35	1.032 ± 0.088	0.373 ± 0.030
	$2\gamma \cdot 0.20$	2864 ± 30	769 ± 75	1043 ± 85	6.20	0.36	1.042 ± 0.086	0.364 ± 0.030
13.84	1γ	85 ± 5	5 ± 14	40 ± 19	4.41	0.26	1.149 ± 1.09	0.469 ± 0.230
	$2\gamma \cdot 0.02$	86 ± 5	13 ± 14	41 ± 19	3.17	0.19	1.136 ± 1.108	0.479 ± 0.228
	$2\gamma \cdot 0.05$	86 ± 5	20 ± 14	41 ± 19	3.42	0.20	1.143 ± 1.095	0.474 ± 0.228
	$2\gamma \cdot 0.20$	84 ± 5	65 ± 14	47 ± 19	3.69	0.22	0.998 ± 1.493	0.572 ± 0.231

TABLE IV: Same as table II, according to Eq. 13, i.e., including also the cubic term, for all considered q^2 values.

q^2 (GeV^2)	case	a_0	a_1	χ^2/N_f
5.4	1γ	46798 ± 182	9627 ± 485	0.11
	$2\gamma \cdot 0.02$	46793 ± 182	9634 ± 485	0.33
	$2\gamma \cdot 0.05$	46794 ± 182	9638 ± 485	0.15
	$2\gamma \cdot 0.20$	46762 ± 182	9635 ± 485	3.66
8.2	1γ	2832 ± 30	1127 ± 85	0.24
	$2\gamma \cdot 0.02$	2859 ± 30	1057 ± 85	0.37
	$2\gamma \cdot 0.05$	2830 ± 30	1065 ± 85	0.59
	$2\gamma \cdot 0.20$	2849 ± 30	1035 ± 85	6.23
13.84	1γ	85 ± 5	40 ± 19	0.25
	$2\gamma \cdot 0.02$	85 ± 5	41 ± 19	0.22
	$2\gamma \cdot 0.05$	85 ± 5	40 ± 19	0.31
	$2\gamma \cdot 0.20$	81 ± 5	43 ± 18	1.37

TABLE V: Results from the linear fit, for different values of q^2 and different TPE contributions, including both $\cos\theta$ and $\cos^3\theta$ terms.

q^2 (GeV^2)	case	a_0	c	a_2	χ^2	χ^2/N_f	$\mathcal{R}$	$\mathcal{A}$
8.2	C=0	2798 ± 959	33 ± 943	1150 ± 636	4.3	0.26	0.986 ± 0.863	0.411 ± 0.267
	C=0.002	2413 ± 947	483 ± 931	1251 ± 629	6.47	0.38	0.860 ± 1.440	0.518 ± 0.330
	C=0.004	2204 ± 938	751 ± 922	1243 ± 624	8.2	0.48	0.806 ± 1.864	0.563 ± 0.371
	C=0.02	1575 ± 905	1602 ± 888	1113 ± 607	8.2	0.49	0.633 ± 4.63	0.706 ± 0.559

TABLE VI: Same as table II,according to Eq. 15.